Original article

Osteopontin silencing attenuates bleomycin-induced murine pulmonary fibrosis by regulating epithelial–mesenchymal transition

Omer Faruk Hatipoglu [a], Eyyup Uctepe [b], Gabriel Opoku [c], Hidenori Wake [a], Kentaro Ikemura [c], Takashi Ohtsuki [c], Junko Inagaki [d], Mehmet Gunduz [e], Esra Gunduz [e], Shogo Watanabe [c], Takashi Nishinaka [a], Hideo Takahashi [a], Satoshi Hirohata [c,*]

[a] *Department of Pharmacology, Faculty of Medicine, Kindai University, Japan*
[b] *Acıbadem Labmed Ankara Tissue Typing Laboratory, Turkey*
[c] *Department of Medical Technology, Graduate School of Health Sciences, Okayama University, Japan*
[d] *Department of Cell Chemistry, Okayama University Graduate School of Medicine, Dentistry and Pharmaceutical Sciences, Okayama University, Japan*
[e] *Department of Otolaryngology, Moriya Keiyu Hospital, Japan*

ABSTRACT

Idiopathic pulmonary fibrosis (IPF) is the most common and most deadly form of interstitial lung disease. Osteopontin (OPN), a matricellular protein with proinflammatory and profibrotic properties, plays a major role in several fibrotic diseases, including IPF; OPN is highly upregulated in patients' lung samples. In this study, we knocked down OPN in a bleomycin (BLM)-induced pulmonary fibrosis (PF) mouse model using small interfering RNA (siRNA) to determine whether the use of OPN siRNA is an effective therapeutic strategy for IPF. We found that fibrosing areas were significantly smaller in specimens from OPN siRNA-treated mice. The number of alveolar macrophages, neutrophils, and lymphocytes in bronchoalveolar lavage fluid was also reduced in OPN siRNA-treated mice. Regarding the expression of epithelial–mesenchymal transition (EMT)-related proteins, the administration of OPN-siRNA to BLM-treated mice upregulated E-cadherin expression and downregulated vimentin expression. Moreover, *in vitro*, we incubated the human alveolar adenocarcinoma cell line A549 with transforming growth factor (TGF)-β1 and subsequently transfected the cells with OPN siRNA. We found a significant upregulation of Col1A1, fibronectin, and vimentin after TGF-β1 stimulation in A549 cells. In contrast, a downregulation of Col1A1, fibronectin, and vimentin mRNA levels was observed in TGF-β1-stimulated OPN knockdown A549 cells. Therefore, the downregulation of OPN effectively reduced pulmonary fibrotic and EMT changes both *in vitro* and *in vivo*. Altogether, our results indicate that OPN siRNA exerts a protective effect on BLM-induced PF in mice. Our results provide a basis for the development of novel targeted therapeutic strategies for IPF.

1. Introduction

Idiopathic pulmonary fibrosis (IPF), one of the most common interstitial lung diseases, is characterized by alveolar epithelial cell injury, extensive fibroblast proliferation, extracellular matrix accumulation in the lung, and irreversible decline in lung function [1]. The incidence of IPF in North America and Europe is 3–9 cases per 100,000 person-years

[2]. The prognosis for patients with IPF is poor, and the median survival of patients with IPF is only 3–5 years [2,3]. Recently, pirfenidone and nintedanib have been used in the treatment of IPF patients; however, the treatment of IPF and disease survival rates have not significantly changed [4,5]. Strong side effects such as diarrhea, vomiting, weight loss, and loss of appetite have been reported for these drugs [6]. According to the American Thoracic Society and the European Respiratory

Society, aside from oxygen therapy and lung transplantation, there are no other proven curative therapies for IPF [7].

Small interfering RNA (siRNA), which can attain target-specific gene silencing, may be a potent tool for gene therapy [8]. A large number of *in vitro* and *in vivo* preclinical studies and recent clinical trials have demonstrated the therapeutic effects of siRNA and provided a completely different direction to conventional treatment methods [9]. The use of siRNA provides new hope for patients, and clinical trials with siRNA are currently underway for various diseases [10]. Many studies that propose the use of siRNA in certain lung diseases continue to be in the preclinical, phase 1, phase 2 and phase 3 stages [11]. However, thus far, no studies have targeted the osteopontin (OPN) gene *in vivo* with siRNA for the treatment of IPF. There are several ways to deliver siRNA into the patient's system. Intranasal administration of siRNA has been demonstrated to be an effective way for delivering siRNA [12] as we carried out in this study.

Epithelial–mesenchymal transition (EMT) is a process in which epithelial cells lose epithelial proteins and recent findings suggest that it may be one possible etiology of IPF, mediated by transforming growth factor beta(TGF)-β1 [13,14].

OPN has been shown to have both proinflammatory and profibrotic properties, and some studies have reported the increased expression of OPN in mouse models of pulmonary fibrosis and patients with chronic lung diseases such as IPF [15]. However, it is still unknown whether OPN siRNA can improve pulmonary fibrosis and EMT both *in vivo* and *in vitro*.

In this study, we investigated whether OPN participates in either TGF-β1- (*in vitro*) or BLM-induced gene regulation (*in vivo*) in pulmonary EMT or fibrosis and whether this function contributes to increased fibrosis in IPF. We also examined the effects of OPN RNA silencing in a BLM-induced IPF mouse model and an *in vitro* TGF-β1-induced EMT model.

2. Materials and methods

2.1. Materials

All reagents were purchased from Sigma-Aldrich (St. Louis, MO, USA) unless otherwise specified. Recombinant human TGF-β1 was purchased from R&D Systems (Minneapolis, MN, USA). Bleomycin was purchased from Nippon Kayaku (Tokyo, Japan). We obtained siRNA DharmaFECT™ and siRNA Transfection Reagent from Dharmacon (Lafayette, CO, USA). Anti-E-cadherin (ab11512), anti-vimentin (ab92547), anti-collagen I (ab21286), and anti-fibronectin (ab2413) antibodies were purchased from Abcam Ltd. (Cambridge, UK). A mouse monoclonal antibody against β-actin (A2228) was purchased from Sigma-Aldrich (Taufkirchen, Germany). Anti-phospho-p38 (#9211), p38 MAPK antibody (#9212), phospho-Smad 2/3 (#8828), and total Smad 2/3 (#8685) were obtained from Cell Signaling Technology, Inc. (Danvers, MA, USA). Rabbit anti-mouse immunoglobulin-horse radish peroxidase (HRP), rabbit anti-goat immunoglobulin-HRP, and goat anti-rabbit immunoglobulin-HRP were purchased from Dako UK Ltd. (Cambridgeshire, UK). Protease inhibitor cocktail was obtained from Roche Diagnostics Ltd. (Sussex, UK). The BCA protein assay kit was purchased from Thermo Fisher Scientific (San Jose, CA, USA). Polyvinylidene difluoride (PVDF) membranes were obtained from GE Healthcare UK Ltd. (Amersham, Buckinghamshire, UK). TRIzol for RNA extraction was obtained from Invitrogen (Carlsbad, CA, USA). The Takara RNA PCR kit was purchased from Takara Shuzo Co., Ltd. (Shiga, Japan). Sequences of siRNAs and quantitative reverse transcription-polymerase chain reaction (RT-qPCR) primers used in the study are shown in Table 1.

2.2. Animals

We used 8–10-week-old C57/BL6 male mice in this study, who were maintained in an accredited, specific pathogen-free, and environmentally controlled facility at the Animal Facility Center of Dişkapi Yildirim Beyazit Training and Research Hospital. This study was approved by the Dişkapi Yildirim Beyazit Training and Research Hospital, Ankara, Turkey under registration number 2013/21. All protocols involving experimental animals followed the local institutional guidelines for animal care, which are comparable to those in the "Guide for the Care and Use of Laboratory Animals" published by the Institute for Laboratory Animal Research (National Institutes of Health Publication No. 8023, revised 1978).

2.3. Bleomycin-induced pulmonary fibrosis and administration of siRNAs in vivo

The fibrotic models used in this study are the popular BLM-induced pulmonary fibrosis mouse models. All animals were divided randomly into three groups: the (a) saline (b) BLM + scramble siRNA and (c) BLM + OPN siRNA groups. To facilitate BLM administration, animals were anesthetized with an intraperitoneal injection of pentobarbital sodium (50 mg/kg) and then administered 2 U/kg BLM dissolved in 50 μL sterile isotonic saline through the intratracheal route using a 22 G plastic

Table 1
Sequence of sense siRNA and qPCR primers.

Target	Species	Forward (5'–3')	Rewerse (5'–3')
Primers for qPCR			
E-cadherin	Human	TATTCCTCCCATCAGCTGCC	CTGTCACCTTCAGCCATCCT
COL1A1	Human	GTGACGAGACCAAGAACTGC	CTGTCCAGGGATGCCATCTC
OPN	Human	CAGCCAGGACTCCATTGACT	ACACTATCACCTCGGCCATC
Fibronectin	Human	AGAATGTCAGCCCACCAAGA	GCTTCTGACATCTGGCTTGA
Vimentin	Human	GCTTCGCCAACTACATCGAC	TTGTCGTTGGTTAGCTGGTC
GAPDH	Human	GAAGGTGAAGGTCGGAGTCA	TGACAAGCTTCCCGTTCTCA
E-cadherin	Mouse	GAATGACAACAGGCCAGAGT	CAGCGTTGTAGGTGTTGACG
Vimentin	Mouse	TGAAGGAAGAGATGGCTCGT	TTGAGTGGGTGTCAACCAGA
IL-6	Mouse	AGCCAGAGTCCTTCAGAGAGA	GGATGGTCTTGGTCCTTAGCC
Fibronectin	Mouse	GAAGAGTGAGCCCCTGATTG	TCATACCCAGGGTTGGTGAT
GAPDH	Mouse	CATGGCCTTCCGTGTTCCTA	TGCCTGCTTCACCACCTTCT
siRNA (Pool)		**siRNA sequence**	
OPN	Human	CCAAGUAAGUCCAACGAAA	
		CAUCUUCUGAGGUCAAUUA	
		UGAACGCGCCUUCUGAUUG	
		GAUGAACUGGUCACUGAUU	
OPN	Mouse	CAGUCGGAUGUGAUCGAUA	
		CCACAUGGACGACGAUGAU	
		CGGAUGAAUCUGACGAAUC	
		GAUCAGGACAACAACGGAA	

cannula. Sterile saline was administered to control mice. Next, on day 3 and 7 after BLM injection, mice with pulmonary fibrosis were intranasally injected with either saline and scramble siRNA or OPN siRNA (2 mg/kg), which was dissolved in diethylpyrocarbonate (DEPC)-treated water mixed with DharmaFECT™ siRNA transfection reagent, to a total volume of 50 μL. On day 14 after BLM administration, the mice were sacrificed; then, lung tissue and 1.5 mL bronchoalveolar lavage fluid (BALF) (0.9% saline, administered through a tracheal cannula, was used to lavage the mouse lungs three times) was collected from each mouse for the experiments (Supplemental Fig. 1A).

2.4. Histological analysis

Histological analysis was performed as previously described [16]. The lung tissue samples were fixed in 4% formalin and embedded in paraffin. Paraffin Section (5 μm thick) were obtained from the fixed lungs and stained with hematoxylin and eosin (HE), Masson's trichrome (MT), and picrosirius red (PSR) (Polysciences Inc., Warrington, PA, USA) stain to determine fibrosis. Lung fibrosis was measured using quantitative histology following Ashcroft's method [17], and the percentage of alveolar air area was calculated as described previously [18]. The tissue sections were examined under a Biozero BZ-X700 microscope (KEYENCE, Tokyo, Japan) at the Central Research Laboratory, Okayama University Medical School, Japan.

2.5. Sodium dodecyl sulfate-polyacrylamide gel electrophoresis (SDS-PAGE) and western blotting

Western blotting was performed as described previously [19]. Briefly, the cells or lungs were washed once in phosphate buffer saline (PBS) and collected by scraping into a 100 μL ice-cold mixture of 50 mM HEPES, 100 mM sodium fluoride, 2 mM sodium orthovanadate, 4 mM ethylenediaminetetraacetic acid (EDTA), 1% Tween-20, 0.1% SDS, and a complete protease inhibitor, and then incubated on ice for 30 min. The supernatant was collected after centrifugation at $13,000 \times g$ for 15 min at 4 °C. Total protein concentration was measured using the BCA protein assay kit with bovine serum albumin as the standard protein. The protein preparations were mixed with 4X Laemmli loading buffer and heated to 95 °C for 5 min. Protein samples (15 μg/well) were loaded for each lane of 10% SDS–PAGE gels, followed by electrophoresis, and transferred to PVDF membranes. After blocking with 5% skim milk in Tris-buffered saline (TBS) for 1 h, the membranes were incubated overnight at 4 °C with primary antibodies in TBS containing 0.05% Tween-20, followed by incubation with HRP-conjugated secondary antibody. β-actin was used for the control loading. Bands were evaluated using densitometry and the ImageJ software.

2.6. Quantitative reverse transcription-PCR

We extracted RNA with TRIzol as previously described [20,21]. Briefly, the samples were washed three times in PBS. Total RNA was separated from DNA and proteins by adding chloroform and precipitated using isopropanol. The precipitate was washed in 70% ethanol, air-dried, and re-diluted in DEPC-treated distilled water. The RNA quality and concentrations were determined using a NanoDrop 2000 spectrophotometer (Thermo Scientific, Waltham, MA, USA). For RT-PCR, the Takara RNA PCR kit was used as follows: 30 °C for 10 min; 42 °C for 50 min; and 90 °C for 5 min. The thermal cycling conditions were 10 min at 30 °C, 60 min at 42 °C, 5 min at 90 °C, and finally held at 4 °C. The mRNA expression levels of target genes were quantified using RT-PCR (ABI Prism 7700; Applied Biosystems, Waltham, USA) using the comparative $2^{-\Delta\Delta CT}$ method as previously described [22,23].

2.7. Cell culture and transfection of synthetic siRNA

The A549 cells were maintained in low glucose-Dulbecco's modified Eagle medium (DMEM) supplemented with 10% FBS, 100 U/mL penicillin, and 100 μg/mL streptomycin and incubated at 37 °C in a humidified atmosphere containing 5% CO_2 and 95% air, as previously described [24,25]. For transfection, the cells were seeded at 2×10^5 cells/well of six-well plates, incubated in normal medium without antibiotics overnight, and transfected with 25 nM siRNA in Opti-MEM using DharmaFECT reagent according to the manufacturer's instructions, together with a nonspecific control pool of siRNA as negative control.

2.8. Statistical analysis

Statistical analysis was performed using the SPSS 11.5 statistical software. The Student's *t*-test was used to analyze differences between the two groups. We considered P < 0.05 as statistically significant.

3. Results

3.1. Osteopontin siRNA protects against BLM-induced lung fibrosis and ameliorates IL-6 induction

To determine whether OPN siRNA has an antifibrotic effect on BLM-induced pulmonary fibrosis in mice, we carried out histological analysis of their tissue specimens and evaluated their BALF, as BLM-induced lung fibrosis is accompanied by an accumulation of BALF cells (eosinophils, macrophages, and neutrophils). OPN expression increased significantly in the BLM-injected mouse groups compared to that in the control group. When the expression of OPN was downregulated by siRNA, OPN protein expression levels significantly decreased compared to those in the control group (Fig. 1A). The optimal siRNA concentration (2 mg/kg) was determined in the pilot experiment (Supplemental Fig. 4). The body weight of BLM-scramble siRNA mice gradually decreased, whereas BLM-OPN siRNA mice maintained their body weight (Supplemental Fig. 1B). We examined the *in vivo* antifibrotic effects of OPN-siRNA on BLM-induced fibrosis by using HE, MT, and PSR staining. As shown in Fig. 1B, the alveolar walls were severely thickened and diffuse infiltrations of inflammatory cells were evident in the pulmonary interstitium in response to BLM administration. Conversely, the fibrosing areas were significantly smaller in specimens from OPN siRNA-treated mice than in those from other control groups. The macroscopic appearance of the lungs indicated that OPN siRNA protected against BLM lung damage (Supplemental Fig. 1C). Furthermore, MT and PSR staining showed that collagen deposition in the alveolar septum of OPN siRNA-treated mice was reduced compared to that in control siRNA mice. The grade of fibrosis was significantly decreased in OPN-siRNA-treated mice, as evidenced by the Ashcroft score, whereas that of the scramble siRNA-treated mice was markedly increased (Fig. 1C). In addition, BLM induced the loss of air space, but OPN siRNA blocked the loss of air space (Fig. 1D). Moreover, interleukin-6 (IL-6) plays an important role in IPF [26]. We found that the significant increase in fibrosis-related cytokine IL-6 levels in lung tissues with bleomycin-induced pulmonary fibrosis and IL-6 levels were dramatically reduced by OPN siRNA in BLM-treated mice (Fig. 1E).

3.2. Osteopontin siRNA administration ameliorates the number of immune cells in BALF

The total number of BALF cells increased after BLM administration. The total number of BALF cells from OPN siRNA mice was significantly lower than that in scramble siRNA mice. Furthermore, the number of alveolar macrophages, neutrophils, and lymphocytes in BALF was reduced in OPN siRNA-treated mice compared with that in the control mice (Fig. 2).
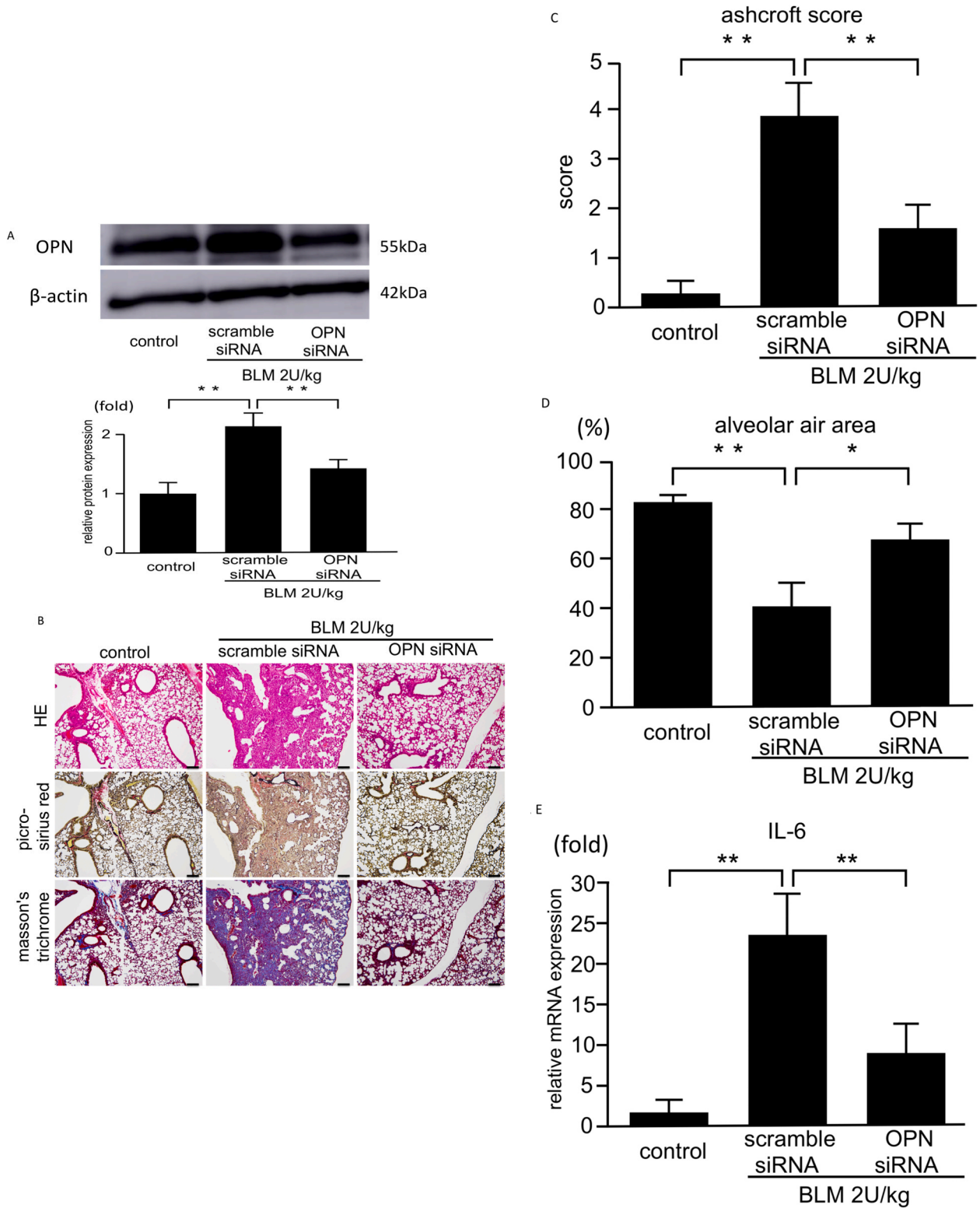
Fig. 1. OPN siRNA attenuates pulmonary fibrosis in BLM-induced pulmonary fibrosis model mice. (A) Increased OPN expression levels in BLM-treated mouse lung tissues collected on day 14. Western blot analysis assessment revealed that upregulation of OPN expression was successfully suppressed by OPN siRNA (n = 3). (B) Histological analysis of mouse lung tissue. Representative images of Hematoxylin and Eosin (HE)-, Masson's Trichrome (MT)-, and Picrosirius Red (PSR)-stained lung sections obtained on day 14. Scale bar = 100 μm. Fibrosing areas were significantly ameliorated in specimens from the OPN-siRNA treated mice than in specimens from BLM-scramble siRNA groups. Degrees of pulmonary fibrosis were scored and evaluated using (C) Ashcroft's method and (D) alveolar air area percentage (n = 5). (E) IL-6 mRNA expression in mouse lung tissues. Data are represented as mean ± SEM. Statistical analysis was carried out using the Student's t-test. P < 0.05 was considered statistically significant (**p < 0.01, *p < 0.05).
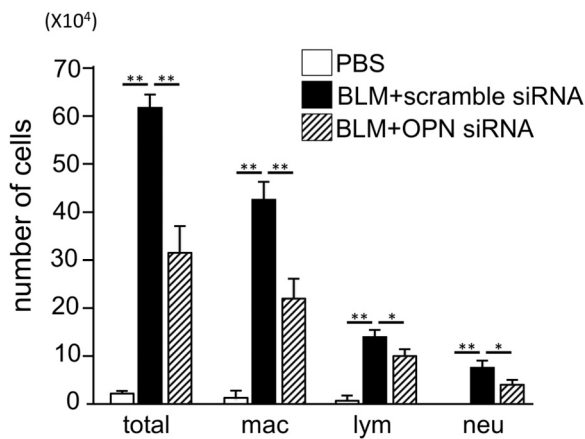
Fig. 2. Effect of OPN siRNA on the infiltration of total and differential cell counts in BALF on day 14 (n = 5–6). Data are represented as mean ± SEM. Statistical analysis was carried out using the Student's *t*-test. P < 0.05 was considered as statistically significant (**p < 0.01, *p < 0.05).

3.3. Osteopontin inhibition attenuates EMT in BLM-treated mice

Next, we examined the expression of EMT-related genes in the lung. The results of the RT-PCR and western blot analysis both indicated that the expression of E-cadherin (epithelial marker) decreased, whereas the expression levels of vimentin and fibronectin (mesenchymal markers) increased with BLM stimulation (Fig. 3A). When the expression of OPN was downregulated by siRNA, it increased the expression of E-cadherin protein and decreased the expression of vimentin (Fig. 3B). The graphs in Fig. 3C and D show the density of each band normalized to β-actin for E-cadherin and vimentin, respectively.

3.4. In vitro OPN inhibition attenuates TGF-β1-dependent EMT activation via Smad signaling

We examined how OPN shows its effect on fibrosis and EMT pathways in A549 cells.

The mRNA expression of the epithelial marker E-cadherin significantly decreased (Fig. 4A) in a dose-dependent manner (Supplemental Fig. 2A) in the scramble siRNA mice. In contrast, the mRNA expression of the mesenchymal marker vimentin increased (Fig. 4B and Supplemental Fig. 2B) indicating that EMT was induced by TGF-β1 stimulation. In addition, the downregulation of OPN by siRNA led to the recovery of E-cadherin mRNA, and the expression levels of vimentin mRNA were attenuated compared to those in scramble siRNA. To further evaluate the antifibrotic effects of OPN siRNAs on A549 cells, collagen, fibronectin, and vimentin expression was measured using RT-PCR. We confirmed a significant upregulation of Col1A1, fibronectin, and vimentin (Fig. 4B) by TGF-β1, whereas siRNAs of OPN reduced the collagen, fibronectin, and vimentin mRNA expression.

Next, we examined the expression of fibrosis-related genes in A549 cells by western blotting. The protein expression levels of Col1A1 and fibronectin were significantly increased and that of E-cadherin decreased in response to TGF-β1 stimulation. However, OPN siRNA markedly restored the protein expression levels of fibrotic genes to a normal level (Fig. 4C, D).

Furthermore, we investigated whether the Smad 2/3 and p38 signaling pathways were involved in the antifibrosis effect of OPN siRNA. We found that TGF-β1 altered the expression levels of fibrosis-related genes and EMT-related genes in A549 cells through the Smad 2/3 and p38 signaling pathways. In addition, downregulation of the OPN expression by siRNA led to the inactivation of Smad 2/3 and p38 signaling pathways (Fig. 4E, F). These data suggest that the antifibrotic effect of OPN siRNA may be mediated by the inhibition of TGF-β1/Smad
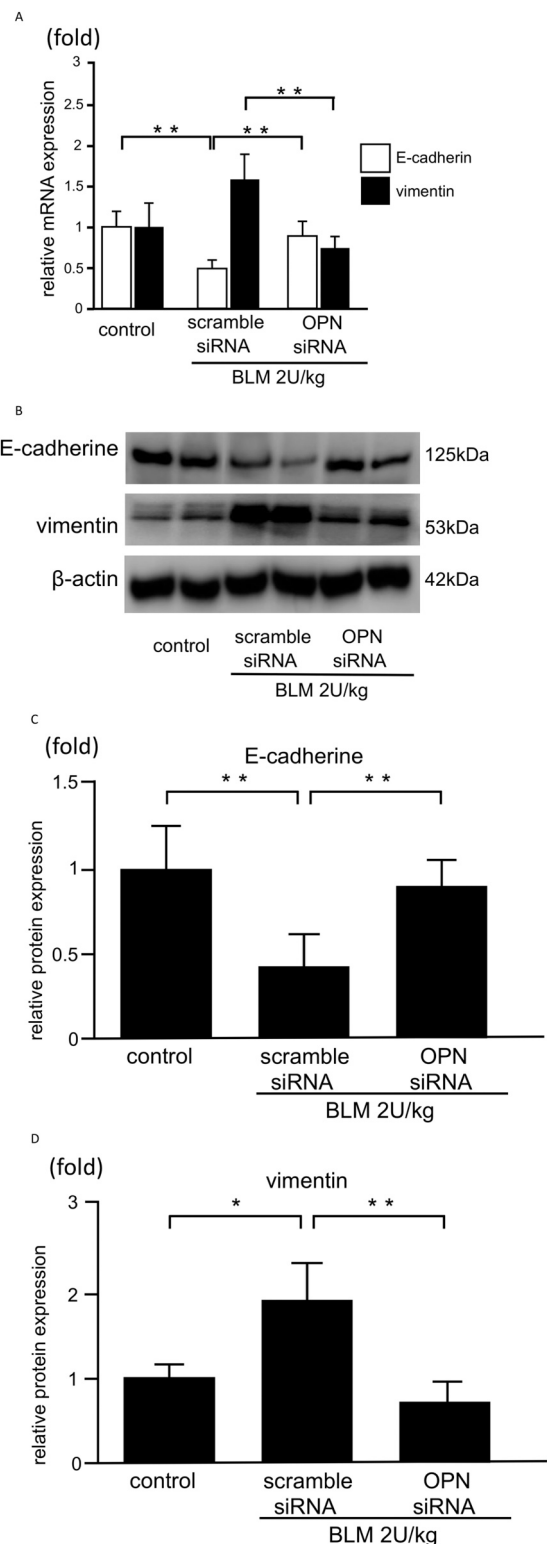

Fig. 3. Effects of OPN siRNA on E-cadherin and vimentin expression in mouse models. (A) E-cadherin and vimentin mRNA and (B) protein expression in mouse lung tissues. (C and D) Western blotting analysis reveals a decrease in E-cadherin (epithelial marker) and concomitant increase in vimentin (mesenchymal marker). β-actin served as loading control for western blotting (n = 3). Data are represented as mean ± SEM. Statistical analysis was carried out using the Student's *t*-test. P < 0.05 was considered statistically significant (**p < 0.01, *p < 0.05).
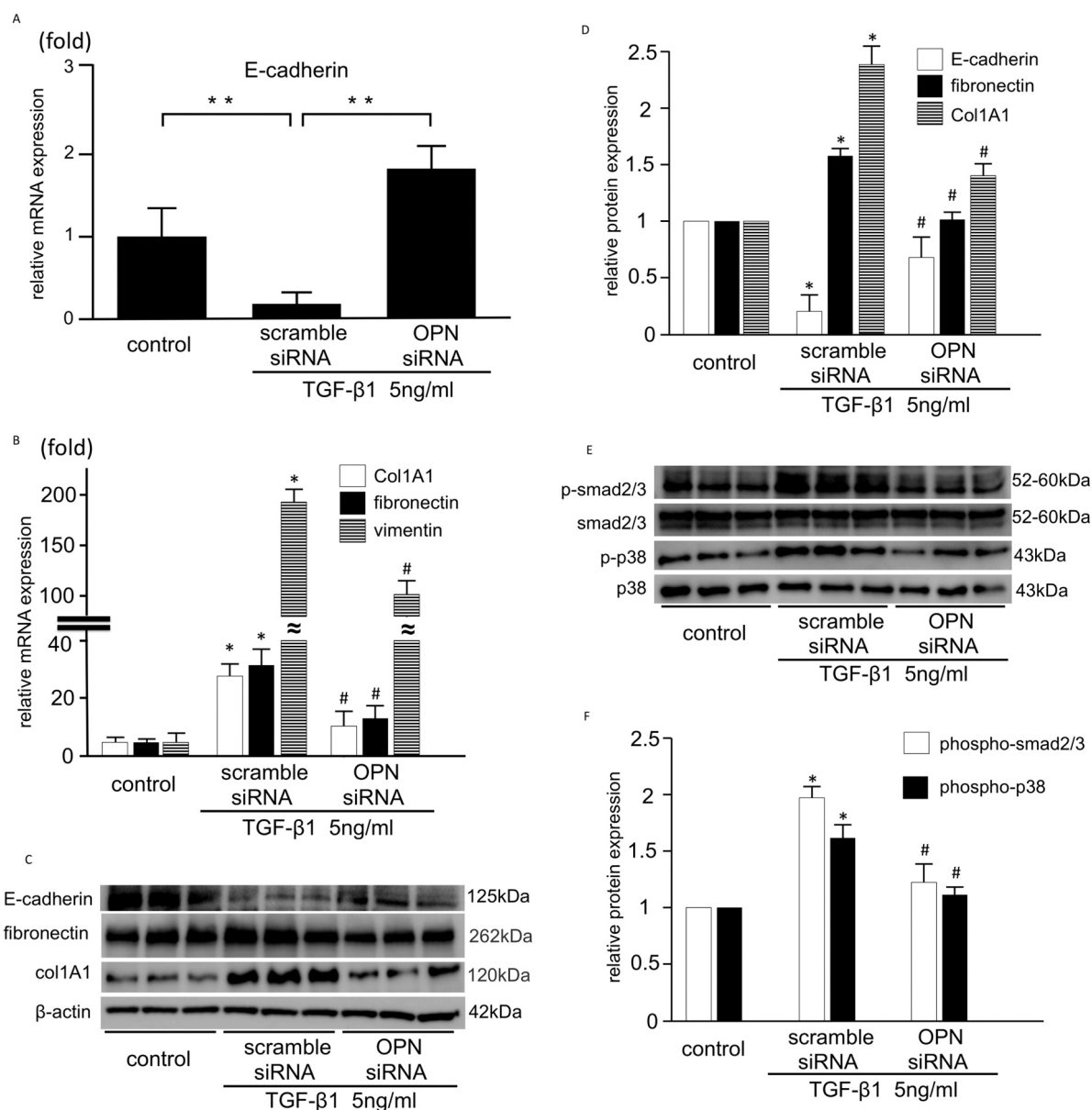
Fig. 4. Analysis for the effect of OPN siRNA on lung fibroblast differentiation and p38, Smad 3/4 signaling after TGF-β1 stimulation. Following the transfection of the A549 cells with the OPN siRNA and TGF-β1 treatment, RT-PCR analysis revealed the expression of (A) E-cadherin, (B) vimentin, COL1A1, and fibronectin. The expression levels were normalized against GAPDH mRNA (n = 5). Data are represented as mean ± SEM. Statistical analysis was carried out using the Student's *t*-test. P < 0.05 was considered statistically significant (*P ≤ 0.05 versus control, #P ≤ 0.05 versus scramble siRNA group). The relative expressions of E-cadherin, fibronectin, and COL1A1 proteins were determined using western blotting (C and D). The activation of p-p38/p38 and p-Smad 3–4/Smad 3–4 protein levels following transfection of the A549 cells with the OPN siRNA and TGF-β1 treatment were determined by western blotting. β-actin was used as a loading control (E and F) (n = 3). Data are represented as mean ± SEM. Statistical analysis was carried out using the Student's *t*-test. P < 0.05 was considered as statistically significant (*P ≤ 0.05 versus control, #P ≤ 0.05 versus scramble siRNA group).

signaling pathway.

Finally, we performed western blotting to examine whether OPN expression was upregulated with TGF-β1 stimulation in an *in vitro* model. Western blot analysis showed that TGF-β1 enhanced the protein level of OPN. When the expression of OPN was downregulated by siRNA, OPN protein expression levels significantly decreased compared with those in the control group (Supplemental Fig. 3).

4. Discussion

In this study, we examined the effects of OPN RNA silencing in a BLM-induced IPF mouse model and an *in vitro* TGF-β1-induced EMT model. The accumulation of lung collagen and infiltration of

inflammatory cells in BALF caused by BLM were significantly attenuated by OPN siRNA. The impact of OPN siRNA was confirmed by the inhibition of EMT in A549 cells. Our data indicated that silencing of OPN attenuated lung fibrosis in BLM-induced IPF model; thus, OPN silencing is a promising therapeutic option for IPF.

IPF is a progressive disease with high mortality rate. Overall, the mean survival rate of IPF patients from its initial diagnosis is approximately 3 years [27]. There are several risk factors such as smoking and potential viral infections (e.g., Epstein–Barr Virus and Herpes simplex virus) [1,28] that are associated with IPF. However, the definitive etiology is still under investigation. In this study, we demonstrated that OPN was upregulated in a BLM-induced IPF model. In clinical IPF, OPN mRNA expression is upregulated [15]. It has also been reported that

serum OPN levels were increased in IPF patients, and the serum level of OPN was linked with acute exacerbation of IPF [29]. These data indicate that OPN is a biomarker for IPF, and our data further support that OPN expression is closely associated with the progression of lung fibrosis in IPF.

Inhibition of lung fibrosis is the key target for the treatment of IPF, because fibrotic change is considered irreversible. The prognosis of IPF worsens in accordance with fibrotic changes. OPN has been reported to be associated with tissue fibrosis [30]. In addition, it has been reported to promote the acetylation of the intracellular high-mobility group box-1 (HMGB1) in hepatic stellate cells and activate the PI3K-pAkt1/2/3 pathway, which results in the increased production of type I collagen [31]. OPN contains several functional domains, such as the RGD domain. Integrin $\alpha v\beta 3$ has been shown to interact through the RGD domain [32,33]. Arriazu et al. reported that OPN also binds to integrin $\alpha v\beta 3$ and activates the PI3K-Akt-IkB-NFkB signaling pathway [34]. Moreover, OPN binds to $\alpha v\beta 6$ integrin [35]. Integrin $\alpha v\beta 6$ is minimally expressed in alveolar epithelial tissues but is highly induced upon lung injury, resulting in lung fibrosis. Integrin $\alpha v\beta 6$ has been demonstrated to be overexpressed in the epithelium of patients with lung sclerosis and pulmonary fibrosis. Horan et al. reported that the partial inhibition of integrin $\alpha v\beta 6$ can effectively inhibit TGF-β activation, epithelial injury, and tissue fibrosis in a murine model of BLM-induced IPF [36]. Munger et al. reported the knockdown of integrin $\beta 6$ in mice to attenuate BLM-induced pulmonary fibrosis and radiation-induced pulmonary fibrosis [37]. Popov et al. reported that integrin $\beta 6$ correlates with the stage of fibrosis in the livers of patients with end-stage liver disease, including chronic hepatitis B and C, primary biliary cholangitis (PBC), and primary sclerosing cholangitis (PSC) [38]. Although we did not examine the distribution of integrin $\alpha v\beta 6$ in our IPF model, the interaction of OPN with integrin $\alpha v\beta 6$ was suggested in these previous studies. The interaction between OPN and integrin $\alpha v\beta 6$ was disturbed by OPN silencing, and this may have resulted in the attenuation of lung fibrosis in the BLM-induced IPF model.

Notably, our results demonstrated that OPN silencing significantly attenuated inflammatory cell infiltration in BALF. Macrophages have been reported to play a role in IPF. Leach et al. reported that endothelial cells facilitate the development of BLM-induced fibrosis through several different mechanisms, contributing to both inflammatory and fibrotic processes. Lund et al. reported that OPN induced inflammatory cell migration and thus mediated chronic inflammation [39]. They also reported that OPN regulates the immune system at different molecular levels (e.g., intracellular and extracellular). In this regard, our results revealed that OPN silencing can effectively attenuate inflammatory reactions by protecting against infiltration of inflammatory cells in BLM-induced IPF models, although the anti-inflammatory molecular mechanism has not been clarified.

Our data demonstrated that silencing of OPN protected from fibrotic changes in BLM-induced IPF model in mice. Notably, this change was accompanied by the inhibition of EMT, which is also known to play a role in tumorigenesis [40,41]. Interestingly, EMT also plays a role in fibrosis [42]. It induces extracellular matrix production, such as collagen, and results in the progression of tissue fibrosis. Recently, EMT alteration has been a found to be a probable event that causes IPF, and EMT plays an important role in the development of IPF [43,44].

EMT is a pathophysiological process in which epithelial cells lose some of their characteristics and markers, including reduced expression of E-cadherin and enhanced expression of vimentin and N-cadherin while showing mesenchymal cell phenotypes. TGF-β1 has been shown to have key roles in pulmonary fibrosis through induction of EMT in alveolar epithelial cells by activating Smad pathways [45]. OPN has also been demonstrated to induce EMT, and several studies have explored this relationship [46,47]. Twist, ZEB, and Snail are the major regulator proteins for EMT, and these molecules have been reported to be regulated by OPN [46]. Although we did not primarily focus on the involvement of these regulatory molecules in this study, OPN silencing attenuated the phosphorylation of the Smad and p38 signaling pathways. Therefore, we consider that OPN silencing affects EMT regulatory molecules (such as Twist, ZEB, and Snail). The precise underlying mechanism will be examined in a future study.

Our data demonstrated that collagen was increased by TGF-β1 at both mRNA and protein levels. Although we did not examine the content of hydroxyproline, many previous studies have demonstrated that hydroxyproline was also increased by TGF-β1 in various cells, including A549 cells [48]. Thus, it can be suggested that hydroxyproline content was also affected by OPN siRNA. Timur et al. reported that OPN enhanced lung fibrosis by promoting TGF-β1 activation, and it may act upstream of TGF-β1 [49]. Another study showed that OPN plays various roles in pulmonary fibrosis, including stimulation of expression and activation of TGF-β1 and induction of fibroblast-to-myofibroblast differentiation. A lack of OPN attenuated TGF-β1 signaling in the lung and reduced pulmonary fibrosis. OPN has been found to be involved in the induction and activation of TGF-β1 signaling *in vivo* and *in vitro*. Moreover, it has been shown that OPN exerts its pro-fibrotic effects by regulating fibroblast and myofibroblast functions through the TGF-β1 pathway [50]. These data strongly support the idea that OPN activates the TGF-β1 signaling pathway.

This is the first study to apply OPN RNA silencing in an IPF model. Although RNA silencing is a mechanism for controlling the target gene, it has never been examined for the treatment of IPF. This method has been approved as a clinical "drug" for a rare inherited disease (hereditary transthyretin-mediated amyloidosis; hATTR amyloidosis). Patisiran, targeting the 3′-untranslated region of transthyretin mRNA, has been reported to reduce the mutant (and wild type) transthyretin protein level [51]. It achieved successful results in the third phase clinical trial [52] and was finally approved by the Food and Drug administration in 2018. In addition, there are various ongoing trials using RNA silencing for cancer therapy. For example, OPN knockdown suppresses the growth and angiogenesis of colon cancer cells [53]. Other researchers also reported that OPN silencing suppresses angiogenesis in endometrial cancer *in vitro* and *in vivo* [54] and reduces liver metastasis in a human pancreatic cancer xenograft model [55]. Therefore, RNA silencing therapy will become a popular option for various diseases in the future, including IPF. Our study sheds light on the challenge of preventing lung fibrosis and inflammatory cell infiltration accompanied by the inhibition of EMT in IPF.

However, this study also has a limitation. It is essential that the effect of OPN silencing does not cause harm to other organs. We did not examine the effect of OPN silencing on other organs assuming that the local administration of the drug to the lung will have a limited effect on other organs.

In conclusion, OPN is a multifunctional protein that plays an important role in the pathogenesis of IPF (Fig. 5. Graphical abstract); thus, OPN silencing is a promising strategy for IPF therapy.

Author contributions

O.F.H., E.U., M.G., and S.H. conceptualized and designed the experiments. O.F.H., E.U., G.O, H.W., K. I., E.G., S.W., J. I. and T.N. performed the experiments. O.F.H., H.T., G.O., H.W., T.O. and S.H. analyzed data. O.F.H. did the statistical analysis. O.F.H. and S.H. wrote the manuscript.
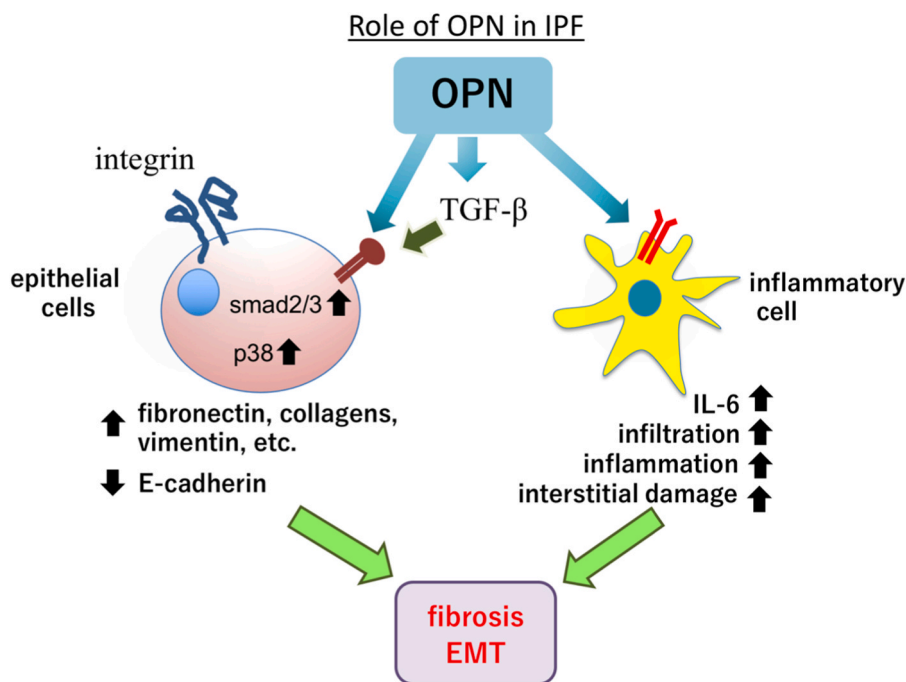
Funding

Fig. 5. Graphic summary of the proposed role of OPN in IPF. Our data suggest that OPN has a diverse function in IPF.

Data availability

The datasets generated for this study are available on request to the corresponding author.

Acknowledgments

Appendix A. Supporting information

Supplementary data associated with this article can be found in the online version at doi:10.1016/j.biopha.2021.111633.

References

[1] G. Raghu, H.R. Collard, J.J. Egan, F.J. Martinez, J. Behr, K.K. Brown, T.V. Colby, J. F. Cordier, K.R. Flaherty, J.A. Lasky, D.A. Lynch, J.H. Ryu, J.J. Swigris, A.U. Wells, J. Ancochea, D. Bouros, C. Carvalho, U. Costabel, M. Ebina, D.M. Hansell, T. Johkoh, D.S. Kim, T.E. King, Y. Kondoh, J. Myers, N.L. Müller, A.G. Nicholson, L. Richeldi, M. Selman, R.F. Dudden, B.S. Griss, S.L. Protzko, H.J. Schünemann, An official ATS/ERS/JRS/ALAT statement: idiopathic pulmonary fibrosis: evidence-based guidelines for diagnosis and management, Am. J. Respir. Crit. Care Med. 183 (2011) 788–824, https://doi.org/10.1164/rccm.2009-040GL.

[2] J. Hutchinson, A. Fogarty, R. Hubbard, T. McKeever, Global incidence and mortality of idiopathic pulmonary fibrosis: a systematic review, Eur. Respir. J. 46 (2015) 795–806, https://doi.org/10.1183/09031936.00185114.

[3] J. Behr, A. Prasse, H. Wirtz, D. Koschel, D. Pittrow, M. Held, J. Klotsche, S. Andreas, M. Claussen, C. Grohé, H. Wilkens, L. Hagmeyer, D. Skowasch, J. F. Meyer, J. Kirschner, S. Gläser, N. Kahn, T. Welte, C. Neurohr, M. Schwaiblmair, T. Bahmer, T. Oqueka, M. Frankenberger, M. Kreuter, Survival and course of lung function in the presence or absence of antifibrotic treatment in patients with idiopathic pulmonary fibrosis: long-term results of the INSIGHTS-IPF registry, Eur. Respir. J. 56 (2020), https://doi.org/10.1183/13993003.02279-2019.

[4] L. Richeldi, V. Cottin, R.M. du Bois, M. Selman, T. Kimura, Z. Bailes, R. Schlenker-Herceg, S. Stowasser, K.K. Brown, Nintedanib in patients with idiopathic pulmonary fibrosis: combined evidence from the TOMORROW and INPULSIS(®) trials, Respir. Med. 113 (2016) 74–79, https://doi.org/10.1016/j. rmed.2016.02.001.

[5] P.W. Noble, C. Albera, W.Z. Bradford, U. Costabel, R.M.D. Bois, E.A. Fagan, R. S. Fishman, I. Glaspole, M.K. Glassberg, L. Lancaster, D.J. Lederer, J.A. Leff, S. D. Nathan, C.A. Pereira, J.J. Swigris, D. Valeyre, T.E. King, Pirfenidone for idiopathic pulmonary fibrosis: analysis of pooled data from three multinational

phase 3 trials, Eur. Respir. J. 47 (2016) 243–253, https://doi.org/10.1183/ 13993003.00026-2015.

[6] V.L.J. Proesmans, M. Drent, M.D.P. Elfferich, P.A.H.M. Wijnen, N.T. Jessurun, A. Bast, Self-reported gastrointestinal side effects of antifibrotic drugs in dutch idiopathic pulmonary fibrosis patients, Lung 197 (2019) 551–558, https://doi.org/ 10.1007/s00408-019-00260-1.

[7] G. Raghu, Idiopathic pulmonary fibrosis: guidelines for diagnosis and clinical management have advanced from consensus-based in 2000 to evidence-based in 2011, Eur. Respir. J. 37 (2011) 743–746, https://doi.org/10.1183/ 09031936.00017711.

[8] C.V. Pecot, G.A. Calin, R.L. Coleman, G. Lopez-Berestein, A.K. Sood, RNA interference in the clinic: challenges and future directions, Nat. Rev. Cancer 11 (2011) 59–67, https://doi.org/10.1038/nrc2966.

[9] R. Kandil, O.M. Merkel, Pulmonary delivery of siRNA as a novel treatment for lung diseases, Ther. Deliv. 10 (2019) 203–206, https://doi.org/10.4155/tde-2019-0009.

[10] R.R. Nikam, K.R. Gore, Journey of siRNA: clinical developments and targeted delivery, Nucleic Acid. Ther. 28 (2018) 209–224, https://doi.org/10.1089/ nat.2017.0715.

[11] B. Hu, L. Zhong, Y. Weng, L. Peng, Y. Huang, Y. Zhao, X.J. Liang, Therapeutic siRNA: state of the art, Sig Transduct. Target Ther. 5 (2020) 101, https://doi.org/ 10.1038/s41392-020-0207-x.

[12] V. Bitko, A. Musiyenko, O. Shulyayeva, S. Barik, Inhibition of respiratory viruses by nasally administered siRNA, Nat. Med. 11 (2005) 50–55, https://doi.org/10.1038/ nm1164.

[13] B.C. Willis, Z. Borok, TGF-beta-induced EMT: mechanisms and implications for fibrotic lung disease, Am. J. Physiol. Lung Cell Mol. Physiol. 293 (2007) 525–534, https://doi.org/10.1152/ajplung.00163.2007.

[14] N. Rout-Pitt, N. Farrow, D. Parsons, M. Donnelley, Epithelial mesenchymal transition (EMT): a universal process in lung diseases with implications for cystic fibrosis pathophysiology, Respir. Res. 19 (2018) 136, https://doi.org/10.1186/ s12931-018-0834-8.

[15] A. Pardo, K. Gibson, J. Cisneros, T.J. Richards, Y. Yang, C. Becerril, S. Yousem, I. Herrera, V. Ruiz, M. Selman, N. Kaminski, Up-regulation and profibrotic role of osteopontin in human idiopathic pulmonary fibrosis, PLoS Med. 2 (2005) 251, https://doi.org/10.1371/journal.pmed.0020251.

[16] K. Asano, C.M. Nelson, S. Nandadasa, N. Aramaki-Hattori, D.J. Lindner, T. Alban, J. Inagaki, T. Ohtsuki, T. Oohashi, S.S. Apte, S. Hirohata, Stromal versican regulates tumor growth by promoting angiogenesis, Sci. Rep. 7 (2017) 17225, https://doi.org/10.1038/s41598-017-17613-6.

[17] T. Ashcroft, J.M. Simpson, V. Timbrell, Simple method of estimating severity of pulmonary fibrosis on a numerical scale, J. Clin. Pathol. 41 (1988) 467–470, https://doi.org/10.1136/jcp.41.4.467.

[18] F. Ruscitti, F. Ravanetti, J. Essers, Y. Ridwan, S. Belenkov, W. Vos, F. Ferreira, A. KleinJan, P. Van Heijningen, C. Van Holsbeke, A. Cacchioli, G. Villetti, F. F. Stellari, Longitudinal assessment of bleomycin-induced lung fibrosis by Micro-CT correlates with histological evaluation in mice, Multidiscip. Respir. Med. 12 (2017) 8, https://doi.org/10.1186/s40248-017-0089-0.

[19] T. Ohtsuki, O.F. Hatipoglu, K. Asano, J. Inagaki, K. Nishida, S. Hirohata, Induction of cemip in chondrocytes by inflammatory cytokines: underlying mechanisms and

potential involvement in osteoarthritis, Int. J. Mol. Sci. 21 (2020), https://doi.org/10.3390/ijms21093140.

[20] O.F. Hatipoglu, T. Miyoshi, T. Yonezawa, M. Kondo, N. Amioka, M. Yoshida, S. Akagi, K. Nakamura, S. Hirohata, H. Ito, Deficiency of CD44 prevents thoracic aortic dissection in a murine model, Sci. Rep. 10 (2020) 6869, https://doi.org/10.1038/s41598-020-63824-9.

[21] T. Ohtsuki, A. Shinaoka, K. Kumagishi-Shinaoka, K. Asano, O.F. Hatipoglu, J. Inagaki, K. Takahashi, T. Oohashi, K. Nishida, K. Naruse, S. Hirohata, Mechanical strain attenuates cytokine-induced ADAMTS9 expression via transient receptor potential vanilloid type 1, Exp. Cell Res. 383 (2019), 111556, https://doi.org/10.1016/j.yexcr.2019.111556.

[22] M. Zeynel Cilek, S. Hirohata, O. Faruk Hatipoglu, H. Ogawa, T. Miyoshi, J. Inagaki, T. Ohtsuki, H. Harada, S. Kamikawa, S. Kusachi, Y. Ninomiya, AHR, a novel acute hypoxia-response sequence, drives reporter gene expression under hypoxia in vitro and in vivo, Cell Biol. Int. 35 (2011) 1–8, https://doi.org/10.1042/cbi20100290.

[23] K.O. Yaykasli, T. Oohashi, S. Hirohata, O.F. Hatipoglu, K. Inagawa, K. Demircan, Y. Ninomiya, ADAMTS9 activation by interleukin 1β via NFATc1 in OUMS-27 chondrosarcoma cells and in human chondrocytes, Mol. Cell. Biochem. 323 (2009) 69–79, https://doi.org/10.1007/s11010-008-9965-4.

[24] J. Inagaki, K. Takahashi, H. Ogawa, K. Asano, O. Faruk Hatipoglu, M. Zeynel Cilek, M. Obika, T. Ohtsuki, M. Hofmann, S. Kusachi, Y. Ninomiya, S. Hirohata, ADAMTS1 inhibits lymphangiogenesis by attenuating phosphorylation of the lymphatic endothelial cell-specific VEGF receptor, Exp. Cell Res. 323 (2014) 263–275, https://doi.org/10.1016/j.yexcr.2014.03.002.

[25] M. Obika, H. Ogawa, K. Takahashi, J. Li, O.F. Hatipoglu, M.Z. Cilek, T. Miyoshi, J. Inagaki, T. Ohtsuki, S. Kusachi, Y. Ninomiya, S. Hirohata, Tumor growth inhibitory effect of ADAMTS1 is accompanied by the inhibition of tumor angiogenesis, Cancer Sci. 103 (2012) 1889–1897, https://doi.org/10.1111/j.1349-7006.2012.02381.x.

[26] T.-T.T. Le, H. Karmouty-Quintana, E. Melicoff, T.-T.T. Le, T. Weng, N.-Y. Chen, M. Pedroza, Y. Zhou, J. Davies, K. Philip, J. Molina, F. Luo, A.T. George, L. J. Garcia-Morales, R.R. Bunge, B.A. Bruckner, M. Loebe, H. Seethamraju, S. K. Agarwal, M.R, Blockade of IL-6 trans signaling attenuates pulmonary fibrosis, J. Immunol. 193 (2014) 3755–3768, https://doi.org/10.4049/jimmunol.1302470.

[27] E.R. Fernández Pérez, C.E. Daniels, D.R. Schroeder, J. Sauver St., T.E. Hartman, B. J. Bartholmai, E.S. Yi, J.H. Ryu, Incidence, prevalence, and clinical course of idiopathic pulmonary fibrosis: a population-based study, Chest 137 (2010) 129–137, https://doi.org/10.1378/chest.09-1002.

[28] Y.W. Tang, J.E. Johnson, P.J. Browning, R.A. Cruz-Gervis, A. Davis, B.S. Graham, K.L. Brigham, J.A. Oates, J.E. Loyd, A.A. Stecenko, Herpesvirus DNA is consistently detected in lungs of patients with idiopathic pulmonary fibrosis, J. Clin. Microbiol. 41 (2003) 2633–2640, https://doi.org/10.1128/JCM.41.6.2633-2640.2003.

[29] X. Gui, X. Qiu, M. Xie, Y. Tian, C. Min, M. Huang, T. Hongyan, T. Chen, X. Zhang, J. Chen, M. Cao, H. Cai, Prognostic value of serum osteopontin in acute exacerbation of idiopathic pulmonary fibrosis, Biomed. Res. Int. (2020), https://doi.org/10.1155/2020/3424208.

[30] S. Zanotti, S. Gibertini, C. di Blasi, C. Cappelletti, P. Bernasconi, R. Mantegazza, L. Morandi, M. Mora, Osteopontin is highly expressed in severely dystrophic muscle and seems to play a role in muscle regeneration and fibrosis, Histopathology 59 (2011) 1215–1228, https://doi.org/10.1111/j.1365-2559.2011.04051.x.

[31] E. Arriazu, X. Ge, T.M. Leung, F. Magdaleno, A. Lopategi, Y. Lu, N. Kitamura, R. Urtasun, N. Theise, D.J. Antoine, N. Nieto, Signalling via the osteopontin and high mobility group box-1 axis drives the fibrogenic response to liver injury, Gut 66 (2017) 1123–1137, https://doi.org/10.1136/gutjnl-2015-310752.

[32] T. Miyoshi, S. Hirohata, H. Ogawa, M. Doi, M. Obika, T. Yonezawa, Y. Sado, S. Kusachi, S. Kyo, S. Kondo, Y. Shiratori, B.G. Hudson, Y. Ninomiya, T. Miyoshi, S. Hirohata, H. Ogawa, M. Doi, M. Obika, T. Yonezawa, Y. Sado, S. Kusachi, S. Kyo, S. Kondo, Y. Shiratori, B.G. Hudson, Y. Ninomiya, Tumor-specific expression of the RGD-α3(IV)NC1 domain suppresses endothelial tube formation and tumor growth in mice, FASEB Journal 20 (11) (2006) 1904–1906, https://doi.org/10.1096/fj.05-5565fje.

[33] J.L. Lee, M.J. Wang, P.R. Sudhir, G. Der Chen, C.W. Chi, J.Y. Chen, Osteopontin promotes integrin activation through outside-in and inside-out mechanisms: OPN-CD44V interaction enhances survival in gastrointestinal cancer cells, Cancer Res. 67 (2007) 2089–2097, https://doi.org/10.1158/0008-5472.CAN-06-3625.

[34] E. Arriazu, M.R. De Galarreta, F.J. Cubero, M. Varela-Rey, M.P.P. De Obanos, T. M. Leung, A. Lopategi, A. Benedicto, I. Abraham-Enachescu, N. Nieto, Extracellular matrix and liver disease, Antioxid. Redox Signal. 21 (2014) 1078–1097, https://doi.org/10.1089/ars.2013.5697.

[35] D.W. Erikson, R.C. Burghardt, K.J. Bayless, G.A. Johnson, Secreted phosphoprotein 1 (SPP1, Osteopontin) binds to integrin Alphavbeta6 on porcine trophectoderm cells and integrin Alphavbeta3 on uterine luminal epithelial cells, and promotes trophectoderm cell adhesion and migration1, Biol. Reprod. 81 (2009) 814–825, https://doi.org/10.1095/biolreprod.109.078600.

[36] G.S. Horan, S. Wood, V. Ona, J.L. Dan, M.E. Lukashev, P.H. Weinreb, K.J. Simon, K. Hahm, N.E. Allaire, N.J. Rinaldi, J. Goyal, C.A. Feghali-Bostwick, E.L. Matteson, C. O'Hara, R. Lafyatis, G.S. Davis, X. Huang, D. Sheppard, S.M. Violette, Partial inhibition of integrin alpha(v)beta6 prevents pulmonary fibrosis without exacerbating inflammation, Am. J. Respir. Crit. Care Med. 177 (2008) 56–65, https://doi.org/10.1164/rccm.200706-805OC.

[37] J.S. Munger, X. Huang, H. Kawakatsu, M.J.D. Griffiths, S.L. Dalton, J. Wu, J. F. Pittet, N. Kaminski, C. Garat, M.A. Matthay, D.B. Rifkin, D. Sheppard, A mechanism for regulating pulmonary inflammation and fibrosis: the integrin αvβ6 binds and activates latent TGF β1, Cell 96 (1999) 319–328, https://doi.org/10.1016/S0092-8674(00)80545-0.

[38] Y. Popov, E. Patsenker, F. Stickel, J. Zaks, K.R. Bhaskar, G. Niedobitek, A. Kolb, H. Friess, D. Schuppan, Integrin alphavbeta6 is a marker of the progression of biliary and portal liver fibrosis and a novel target for antifibrotic therapies, J. Hepatol. 48 (2008) 453–464, https://doi.org/10.1016/j.jhep.2007.11.021.

[39] S.A. Lund, C.M. Giachelli, M. Scatena, The role of osteopontin in inflammatory processes, J. Cell Commun. Signal. 3 (2009) 311–322, https://doi.org/10.1007/s12079-009-0068-0.

[40] L. Larue, A. Bellacosa, Epithelial-mesenchymal transition in development and cancer: role of phosphatidylinositol 3' kinase/AKT pathways, Oncogene 24 (2005) 7443–7454, https://doi.org/10.1038/sj.onc.1209091.

[41] H. Okabe, K. Mima, S. Saito, H. Hayashi, K. Imai, H. Nitta, D. Hashimoto, A. Chikamoto, T. Ishiko, T. Beppu, H. Baba, Epithelial-mesenchymal transition in gastroenterological cancer, J. Cancer Metastasis Treat. (2015), https://doi.org/10.4103/2394-4722.165118.

[42] M. Li, F. Luan, Y. Zhao, H. Hao, Y. Zhou, W. Han, X. Fu, Epithelial-mesenchymal transition: an emerging target in tissue fibrosis, Exp. Biol. Med. 241 (2016) 1–13, https://doi.org/10.1177/1535370215597194.

[43] C. Hill, M. Jones, D. Davies, V. Wang, Epithelial-Mesenchymal Transition Contributes to Pulmonary Fibrosis via Aberrant Epithelial/Fibroblastic Cross-Talk, J. Lung Heal. Dis. 3 (2) (2019) 31–35, https://doi.org/10.29245/2689-999x/2019/2.1149.

[44] F. Salton, M.C. Volpe, M. Confalonieri, Epithelial-mesenchymal transition in the pathogenesis of idiopathic pulmonary fibrosis, Medicina (2019), https://doi.org/10.3390/medicina55040083.

[45] T.L. Hackett, S.M. Warner, D. Stefanowicz, F. Shaheen, D.V. Pechkovsky, L. A. Murray, R. Argentieri, A. Kicic, S.M. Stick, T.R. Bai, D.A. Knight, Induction of epithelial-mesenchymal transition in primary airway epithelial cells from patients with asthma by transforming growth factor-beta1, Am. J. Respir. Crit. Care Med. 180 (2009) 122–133, https://doi.org/10.1164/rccm.200811-1730OC.

[46] A. Kothari, M. Arffa, V. Chang, R. Blackwell, W.-K. Syn, J. Zhang, Z. Mi, P. Kuo, Osteopontin—a master regulator of epithelial-mesenchymal transition, J. Clin. Med. 5 (2016), https://doi.org/10.3390/jcm5040039.

[47] N.Y. Li, C.E. Weber, Z. Mi, P.Y. Wai, B.D. Cuevas, P.C. Kuo, Osteopontin up-regulates critical epithelial-mesenchymal transition transcription factors to induce an aggressive breast cancer phenotype, J. Am. Coll. Surg. (2013), https://doi.org/10.1016/j.jamcollsurg.2013.02.025.

[48] K. Tian, P. Chen, Z. Liu, S. Si, Q. Zhang, Y. Mou, L. Han, Q. Wang, X. Zhou, Sirtuin 6 inhibits epithelial to mesenchymal transition during idiopathic pulmonary fibrosis via inactivating TGF-β1/Smad3 signaling, Oncotarget 8 (2017) 61011–61024, https://doi.org/10.18632/oncotarget.17723.

[49] T.O. Khaliullin, E.R. Kisin, A.R. Murray, N. Yanamala, M.R. Shurin, D.W. Gutkin, L. M. Fatkhutdinova, V.E. Kagan, A.A. Shvedova, Mediation of the single-walled carbon nanotubes induced pulmonary fibrogenic response by osteopontin and TGF-β1, Exp. Lung Res. 43 (2017) 311–326, https://doi.org/10.1080/01902148.2017.1377783.

[50] J. Dong, Q. Ma, Osteopontin enhances multi-walled carbon nanotube-triggered lung fibrosis by promoting TGF-β1 activation and myofibroblast differentiation, Part. Fibre Toxicol. 14 (2017) 18, https://doi.org/10.1186/s12989-017-0198-0.

[51] T. Coelho, D. Adams, A. Silva, P. Lozeron, P.N. Hawkins, T. Mant, J. Perez, J. Chiesa, S. Warrington, E. Tranter, M. Munisamy, R. Falzone, J. Harrop, J. Cehelsky, B.R. Bettencourt, M. Geissler, J.S. Butler, A. Sehgal, R.E. Meyers, Q. Chen, T. Borland, R.M. Hutabarat, V.A. Clausen, R. Alvarez, K. Fitzgerald, C. Gamba-Vitalo, S.V. Nochur, A.K. Vaishnaw, D.W.Y. Sah, J.A. Gollob, O.B. Suhr, Safety and efficacy of RNAi therapy for transthyretin amyloidosis, N. Engl. J. Med. 369 (2013) 819–829, https://doi.org/10.1056/NEJMoa1208760.

[52] D. Adams, A. Gonzalez-Duarte, W.D. O'Riordan, C.C. Yang, M. Ueda, A.V. Kristen, I. Tournev, H.H. Schmidt, T. Coelho, J.L. Berk, K.P. Lin, G. Vita, S. Attarian, V. Planté-Bordeneuve, M.M. Mezei, J.M. Campistol, J. Buades, T.H. Brannagan, B. J. Kim, J. Oh, Y. Parman, Y. Sekijima, P.N. Hawkins, S.D. Solomon, M. Polydefkis, P.J. Dyck, P.J. Gandhi, S. Goyal, J. Chen, A.L. Strahs, S.V. Nochur, M.T. Sweetser, P.P. Garg, A.K. Vaishnaw, J.A. Gollob, O.B. Suhr, Patisiran, an RNAi therapeutic, for hereditary transthyretin amyloidosis, N. Engl. J. Med. 379 (2018) 11–21, https://doi.org/10.1056/NEJMoa1716153.

[53] X.L. Wu, K.J. Lin, A.P. Bai, W.X. Wang, X.K. Meng, X.L. Su, M.X. Hou, P. De Dong, J.J. Zhang, Z.Y. Wang, L. Shi, Osteopontin knockdown suppresses the growth and angiogenesis of colon cancer cells, WJG 20 (2014) 10440, https://doi.org/10.3748/wjg.v20.i30.10440.

[54] X. lian Du, T. Jiang, X. gui Sheng, R. Gao, Q. shui Li, Inhibition of osteopontin suppresses in vitro and in vivo angiogenesis in endometrial cancer, Gynecol. Oncol. (2009), https://doi.org/10.1016/j.ygyno.2009.08.029.

[55] K. Ohno, H. Nishimori, T. Yasoshima, K. Kamiguchi, F. Hata, R. Fukui, K. Okuya, Y. Kimura, R. Denno, S. Kon, T. Uede, N. Sato, K. Hirata, Inhibition of osteopontin reduces liver metastasis of human pancreatic cancer xenografts injected into the spleen in a mouse model, Surg. Today 40 (2010) 347–356, https://doi.org/10.1007/s00595-009-4082-x.